International Journal of Science and Research (IJSR)
ISSN (Online): 2319-7064
Index Copernicus Value (2013): 6.14 | Impact Factor (2013): 4.438

Cause and Catastrophe of Strengthening Mechanisms in 6061/Al_2O_3 Composites Prepared by Stir Casting Process and Validation Using FEA

A. Chennakesava Reddy[1]

Professor, Department of Mechanical Engineering, JNTUH College of Engineering
Kukatpally, Hyderabad – 500 085, Telangana, India

Abstract: ***The present research has been focused to anticipate all these effects in 6061/Al_2O_3 metal matrix composites. It was found that the tensile strength and stiffness increase with increasing volume fraction of Al_2O_3 particulates. The tensile strength and stiffness were decreased with increased size of particulates. After heat treatment to the T4 condition, most of the coarse intermetallic phases such as (Al_2Cu, Mg_2Si) are dissolved to form $Al_5Cu_2Mg_8Si_6$ or $Al_4CuMg_5Si_4$ compound. A clustering of particulates was observed in the composites having very small particles. Formation of Mg_2Si precipitates were also noticed at the matrix/particle interface. The interface between particle and matrix was assumed to be Mg_2Si for the finite element analysis. The proposed formulae by the author for the tensile strength and elastic modulus could predict them very close to the experimental values of 6061/Al_2O_3 composites.***

Keywords: Alumina, 6061, strength, FEA, stiffness, stir casting.

1. Introduction

Metal matrix composite usually consists of a matrix alloy and a discontinuous phase in the form of particulates called the reinforcement. The addition of ceramic particulates into aluminium alloys modify the physical and mechanical properties, promising high specific elastic modulus, strength-to-weight ratio, fatigue strength, and wear resistance. Redsten et al. [1] have investigated the mechanical properties of oxide dispersion strengthened Al containing 25 vol. %, 0.28μm Al_2O_3 particles. They found that the yield strength was low, but 0.2% proof stress and ultimate tensile strength were higher about 200 MPa and 330 MPa respectively. Srivatsan [2] has studied the fracture behaviour of 2011 Al alloy reinforced with two different volume fractions of 10 and 15% Al_2O_3 in order to understand the effects of reinforcement on microstructure, tensile and quasistatic fracture behaviour. He observed that the elastic modulus in 10 and 15 vol. % composites was respectively 10 and 45% more than that of the unreinforced alloy. The tensile strength in the 15 vol. % composite was found to be 2% more than that of the 10 vol. % composite. The tensile fracture surface was observed to be brittle appearance on macroscopic scale and microscopically local ductile and brittle fracture. Fracture of the particles with failure of matrix between particles and decohesion found to occur. Kamat et al. [3] have performed tension, and fracture toughness tests on 2011-O and 2024-O Al alloy reinforced with Al_2O_3 having 2 to 20 % volume fraction with different particle sizes. They have observed that yield strength was increased with decrease in spacing between particles. Pestes et al. [4] have studied the effect of particle size from 3-165 μm on the fracture toughness of Al/Al_2O_3 composites with the volume fraction ranging from 45-54%. Fracture toughness found to be dependent on the inter-particle spacing provided that the particles were below a critical size. Increasing inter-particle spacing can increase the toughness either by decreasing the volume fraction of particulates or increasing size of the particles. When metal matrix composites are manufactured through casting route, there is every possibility of porosity in the composites, improper wettability and particle clustering.

All these phenomena may influence the tensile strength and stiffness of composite. With this underlying background, the motivation for this article was to study the influence of volume fraction and particle size of Al_2O_3 reinforcement, clustering of particles, the formation of precipitates at the particle / matrix interface, cracking of particles, and voids/porosity on the elastic modulus and tensile strengths of 6061/Al_2O_3 metal matrix composites.

2. Analytical Models

For a tensile testing of a rectangular cross-section, the tensile strength is given by:

$$\sigma_t = \frac{F_t}{A_t} \tag{1}$$

The engineering strain is given by:

$$\varepsilon_t = \frac{\Delta L_t}{L_{to}} = \frac{L_t - L_{to}}{L_{to}} \tag{2}$$

where ΔL_t is the change in gauge length, L_0 is the initial gauge length, and L_t is the final length, F_t is the tensile force and A_t is the nominal cross-section of the specimen.

The Weibull cumulative distribution can be transformed so that it appears in the familiar form of a straight line: $Y = mx + b$ as follows:

$$F(x) = 1 - \exp\left(-\left(\frac{x}{\alpha}\right)^{\beta}\right) \tag{3}$$

$$1 - F(x) = \exp\left(-\left(\frac{x}{\alpha}\right)^{\beta}\right)$$

$$\ln\left[\ln\left(\frac{1}{1-F(x)}\right)\right] = \beta \ln x - \beta \ln \alpha \tag{4}$$

Comparing this equation with the simple equation for a line, we see that the left side of the equation corresponds to *Y*, ln*x* corresponds to *X*, β corresponds to m, and -βlnα corresponds to *b*. Thus, when we perform the linear regression, the estimate of the Weibull parameter (β) comes directly from the slope of the line. The estimate of the parameter (α) must be calculated as follows:

$$\alpha = \exp\left(-\left(\frac{b}{\beta}\right)\right) \quad (5)$$

According to the Weibull statistical-strength theory for brittle materials, the probability of survival, *P* at a maximum stress (σ) for uniaxial stress field in a homogeneous material governed by a volumetric flaw distribution is given by

$$P(\sigma_f \geq \sigma) = R(\sigma) = \exp(-B(\sigma)) \quad (6)$$

where σ_f is the value of maximum stress of failure, *R* is the reliability, and β is the risk of rupture. A non-uniform stress field (σ) can always be written in terms of the maximum stress as follows:

$$\sigma(x, y, z) = \sigma_{0f}(x, y, z) \quad (7)$$

For a two-parameter Weibull model, the risk of rupture is of the form

$$B(s) = A\left(\frac{\sigma}{\sigma_0}\right)^{\beta} \quad (\sigma_0, \beta > 0) \quad (8)$$

$$\text{where } A = \int_v [f(x, y, z)]^{\beta} dv \quad (9)$$

and σ_0 is the characteristic strength, and β is the shape factor that characterizes the flaw distribution in the material. Both of these parameters are considered to be material properties independent of size. Therefore, the risk to break will be a function of the stress distribution in the test specimen. Equation (8) can also be written as

$$B(\sigma) = \left(\frac{\sigma}{\sigma_A}\right)^{\beta} \quad (10)$$

$$\sigma_A = \sigma[A]^{-\frac{1}{\beta}} \quad (11)$$

And the reliability function, Eq. (11) can be written as a two-parameter Weibull distribution

$$R(\sigma) = e^{-\left(\frac{\sigma}{\sigma_A}\right)^{\beta}} \quad (12)$$

The tensile tests of specimens containing different stress fields can be represented by a two-parameter Weibull distribution with the shape parameter and characteristic strength. The author has proposed expression for the tensile strength considering the effects of reinforced particle size and voids/porosity. The expression of tensile strength is given below:

$$\sigma_t = \sigma_o[V_m + V_p - V_v]^{-1/\beta} \quad (\sigma_0, \beta_t > 0) \quad (13)$$

where σ_0 is the characteristic strength of tensile loading, β is the shape parameter which characterize the flaw distribution in the tensile specimen, V_m, V_p, and V_v are respectively volume of the matrix, volume of the reinforced particles and volume of the voids/porosity in the tensile specimen.

3. Experimental Procedure

The composites were prepared by the stir casting and low-pressure die casting process. The matrix alloy was 6061. The reinforcement was Al_2O_3 particulates. The volume fractions of Al_2O_3 reinforcement are 12%, 16%, and 20%. The particle sizes of Al_2O_3 reinforcement are 2μm, 5μm, and 10 μm.

3.1 Preparation of Melt and Metal Matrix Composites

The 6061 matrix alloy was melted in a resistance furnace. The crucibles were made of graphite. The melting losses of the alloy constituents were taken into account while preparing the charge. The charge was fluxed with coverall to prevent dressing. The molten alloy was degasified by tetrachlorethane (in solid form). The crucible was taken away from the furnace and treated with sodium modifier. Then the liquid melt was allowed to cool down just below the liquidus temperature to get the melt semi solid state. At this stage, the preheated (500^0C for 1 hour) reinforcement particles were added to the liquid melt. The molten alloy and reinforcement particles are thoroughly stirred manually for 15 minutes. After manual steering, the semi-solid, liquid melt was reheated, to a full liquid state in the resistance furnace followed by an automatic mechanical stirring using a mixer to make the melt homogenous for about 10 minutes at 200 rpm. The temperature of melted metal was measured using a dip type thermocouple. The preheated cast iron die was filled with dross-removed melt by the compressed (3.0 bar) argon gas [5, 6].

3.2 Heat Treatment

Prior to the machining of composite samples, a solution treatment was applied at 500^0 C for 1 hour, followed by quenching in cold water. The samples were then naturally aged at room temperature for 100 hours.

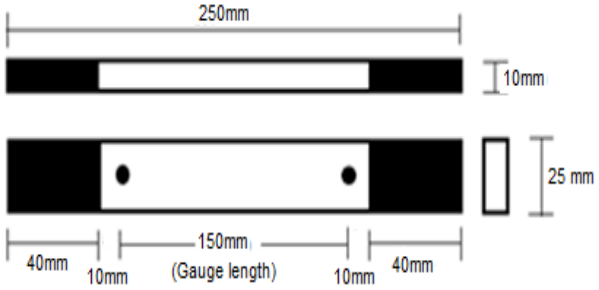

Figure 1: Shape and dimensions of tensile specimen

3.3 Tensile tests

The heat-treated samples were machined to get flat-rectangular specimens (figure 1) for the tensile tests. The tensile specimens were placed in the grips of a Universal Test Machine (UTM) at a specified grip separation and pulled until failure. The test speed was 2 mm/min (as for ASTM D3039). A strain gauge was used to determine elongation.

3.4 Optical and scanning electron microscopic analysis

An image analyser was used to study the distribution of the reinforcement particles within the 6061 aluminium alloy matrix. The polished specimens were ringed with distilled water, and etched with 0.5% HF solution for optical microscopic analysis. Fracture surfaces of the deformed/fractured test samples were analysed with a scanning electron microscope (SEM) to define the macroscopic fracture mode and to establish the microscopic mechanisms governing fracture. Samples for SEM observation were obtained from the tested specimens by sectioning parallel to the fracture surface and the scanning was carried using S-3000N Toshiba SEM.

3.5 Finite element analysis

Particle distribution, clustering and porosity in the composite were modeled using ANSYS software. A test coupon of 0.03mm x 0.03mm composite was modelled to examine particle clustering, debonding. In addition, a porosity of 42µm was modeled in the test coupon of 0.1mm x 0.1mm. A triangle element of 6 degrees of freedom was used to mesh the Al_2O_3 particle and the matrix alloy [7]. The interface between particle and matrix was assumed to be Mg_2Si. For load transfer from the matrix to the particle point-to-point coupling of zero length was used. The test coupon was tensile loaded.

4. Results and Discussion

The modulus of elasticity is the stiffness of the composite. The modulus of elasticity is improved by the addition of Al_2O_3 particles. The composites can fail on the microscopic or macroscopic scale. The tensile strength is the maximum stress that the material can sustain under a uniaxial loading. For metal matrix composites, the tensile strength depends on the scale of stress transfer from the matrix to the particulates.

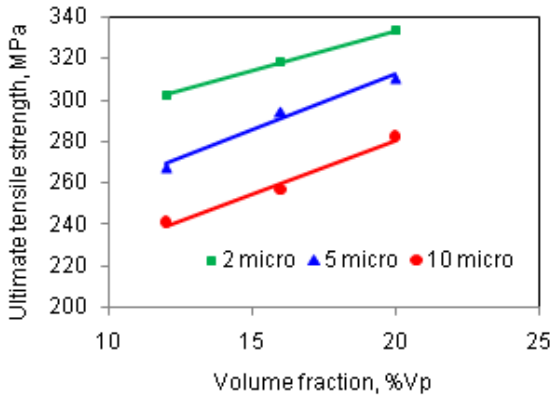

Figure 2: Variation of the tensile strength with the volume fraction and particle size of Al_2O_3

4.1 Cause of strengthening mechanisms

The variation of tensile strength with volume fraction and particle size is shown in figure 2. It is obviously shown that, for a given particle size the tensile strength increases with an increase in the volume fraction of Al_2O_3. As the particle size decreases the tensile strength increases. This is due to fact that the smaller particles have a larger surface area for transferring stress from the matrix. The other possibility, of increasing strength is owing to the formation of precipitates at the particle/matrix interface.

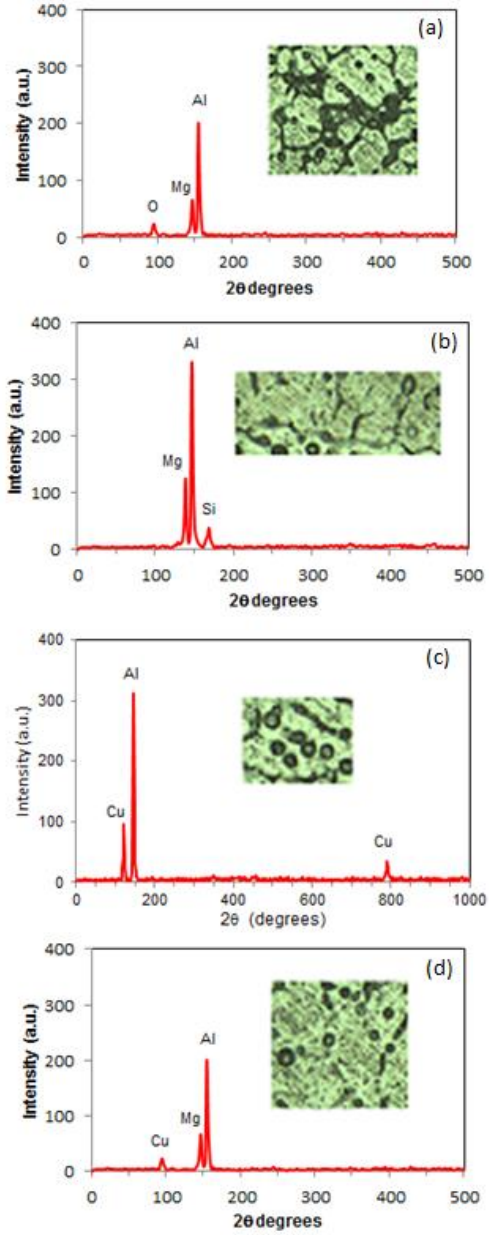

Figure 3: EDS analysis of heat-treated 6061/Al_2O_3 metal matrix composite (Al_2O_3 particle size =10µm and Vp = 20%).

EDX spectrum (figure 3a) shows isolated Magnesium-rich particles (suspected to be $MgA1_2O_4$ spinel or MgO). The intermetallic phases of Mg_2Si or Al-Mg-Si ternary alloys are formed at the particle/matrix interface as shown in figure 3b. The precipitates of Al_2Cu are observed over the grains as shown in figure 3c. Very small precipitates of Al-Mg-Cu are also seen as in the interior of the grains (figure 3d). The EDX spectrums depict the possibility of formation of intermetallic particles $Al_5Cu_2Mg_8Si_6$ or $Al_4CuMg_5Si_4$. The grains are also found to be refined due to the heat-treatment. After heat treatment to the T4 condition, most of the coarse intermetallic phases such as (Al_2Cu, Mg_2Si) are dissolved to form $Al_5Cu_2Mg8Si6$ or $Al_4CuMg_5Si_4$ compound; however residual amounts remain. The agglomerations appear to be

well bonded to the matrix. Due to solution treatment the oxide film at the interface between matrix and reinforced particles turns into fine particles ($MgAl_2O_4$).

The precipitation hardening also influences the direct strengthening of the composite due to heat treatment. An increase in volume fraction with smaller particles of Al_2O_3 increases the amount of strengthening owing to increasing obstacles to the dislocations. This is because, smaller particle size means a lower inter-particle spacing so that nucleated voids in the matrix are unable to coalesce as easily.

4.2 Catastrophe of strengthening mechanisms

As the particle size increases the tensile strength decreases as shown in figure 2. The coarser particles were more likely to contain flaws, which might severely reduce their strength than smaller particles [8].

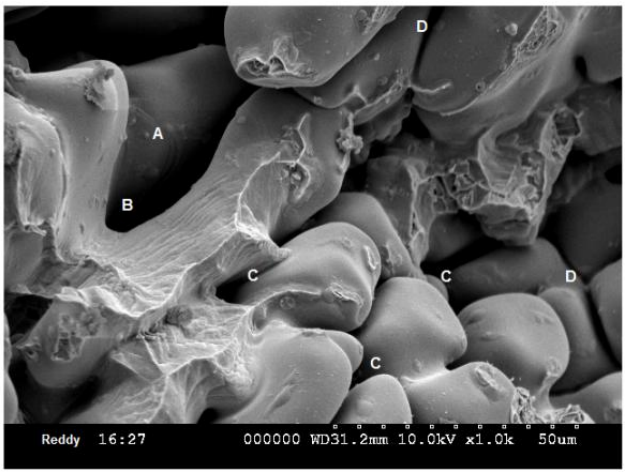

Figure 4: Cracking of Al_2O_3 particle of 30µm size

Non-planar cracking (A) of particle (figure 4) is observed in the $6061/Al_2O_3$ composite comprising 10µm particles. This is because of the low passion's ratio (0.21) of Al_2O_3 particle as than that (0.33) of the matrix alloy. Finite element model of test coupon of size 0.03mm x 0.03mm consisting of particles of size of 10µm is shown figure 5a. The volume fraction of Al_2O_3 is nearly 28%. The interface (very narrow around the particle) between 6061 and Al_2O_3 particles is considered as Mg_2Si. The maximum tensile strength is 310.56 MPa (figure 5b) whereas the experimental value is 310.12 MPa. This is error is due to assumption of uniform distribution of particles in the matrix. The maximum stress-intensity values are found to be at the particle/matrix interface (figure 5c) where the debonding (D) occurs as shown in figure 4. The same kind of phenomena is observed with strain-intensity values (figure 5d) at the particle/matrix interface. The zones of matrix are in safe limits. The Al_2O_3 particle experiences compressive stress in the transverse direction of tensile loading. The transverse movement is higher in the outer region than in the inner region of the specimen.

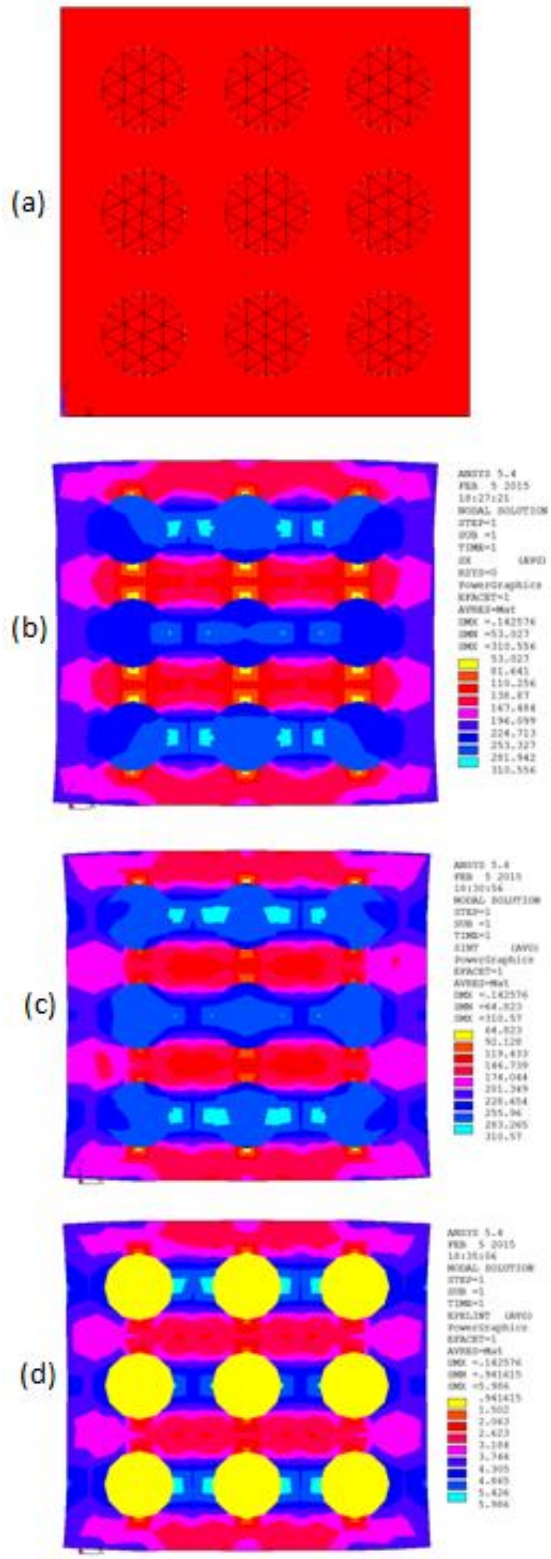

Figur 5: Finite element analysis of composite with particle distribution

There is every possibility of cavity formation (C) during the preparation of composite or during testing of composite due to debonding (D) as shown in figure 4. The porosity (B as shown in figure 4) of approximately 48µm is also revealed in the $6061/Al_2O_3$ composite having 10µm particles as shown in figure 6a. Finite element model of test coupon of size 0.1mm x 0.1mm consisting of particles of size of 10µm is shown figure 6b. The loss of strength due to porosity is nearly 40 MPa.

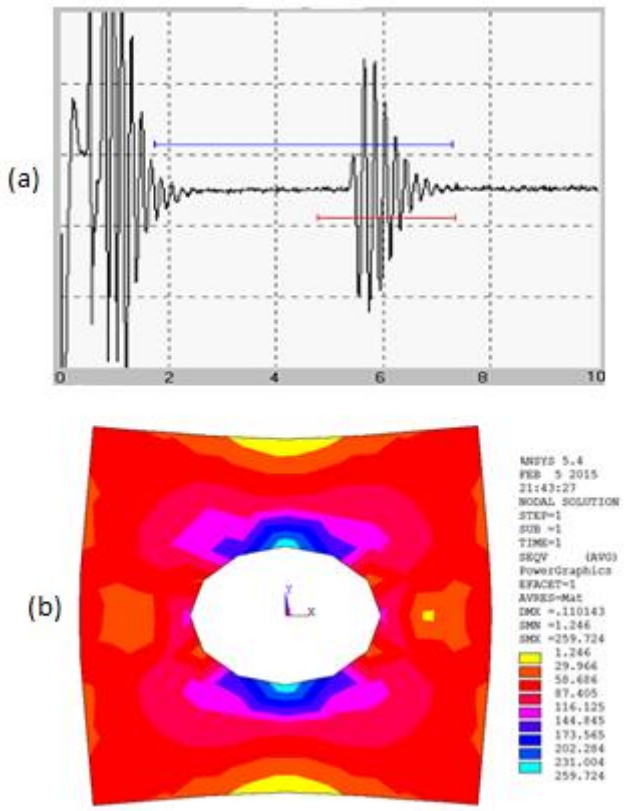

Figure 6: Porosity in 6061/Al_2O_3 composite (particles of 10µm size and Vp = 20%)

There is a possibility of clustering (E) of Al_2O_3 particles as seen in figure 4. These clusters act as sites of stress concentration. At higher volume fractions the particle-particle interaction may develop clustering in the composite. The formation of clustering increases with an increase in the volume fraction and with a decrease in the particle size. A five-particle clustering is modeled in ANSYS as shown in figure 7a. The maximum stress intensity is observed at the center particle and at the connectivity of adjacent particles with center particle in the direction of tensile loading as seen figure 7b. The maximum strain intensity is also observed at the clustering interface of particles as seen in figure 7c.

4.3 Strengthening Mechanisms

The strength of a particulate metal matrix composite depends on the strength of the weakest zone and metallurgical phenomena in it. Even if numerous theories of composite strength have been published, none is universally taken over however. Along the path to the new criteria, we attempt to understand them.

For very strong particle-matrix interfacial bonding, Pukanszky et al. [9] presented an empirical relationship as given below:

$$\sigma_c = \left[\sigma_m \left(\frac{1-v_p}{1+2.5v_p}\right)\right] e^{Bv_p} \quad (14)$$

where B is an empirical constant, which depends on the surface area of particles, particle density and interfacial bonding energy. The value of B varies between from 3.49 to 3.87. The strength values obtained from this criterion are approaching the experimental values of the composites as shown in figure 8. This criterion has taken care of the presence of particulates in the composite and interfacial bonding between the particle/matrix. The effect of particle size and voids/porosity were not considered in this criterion.

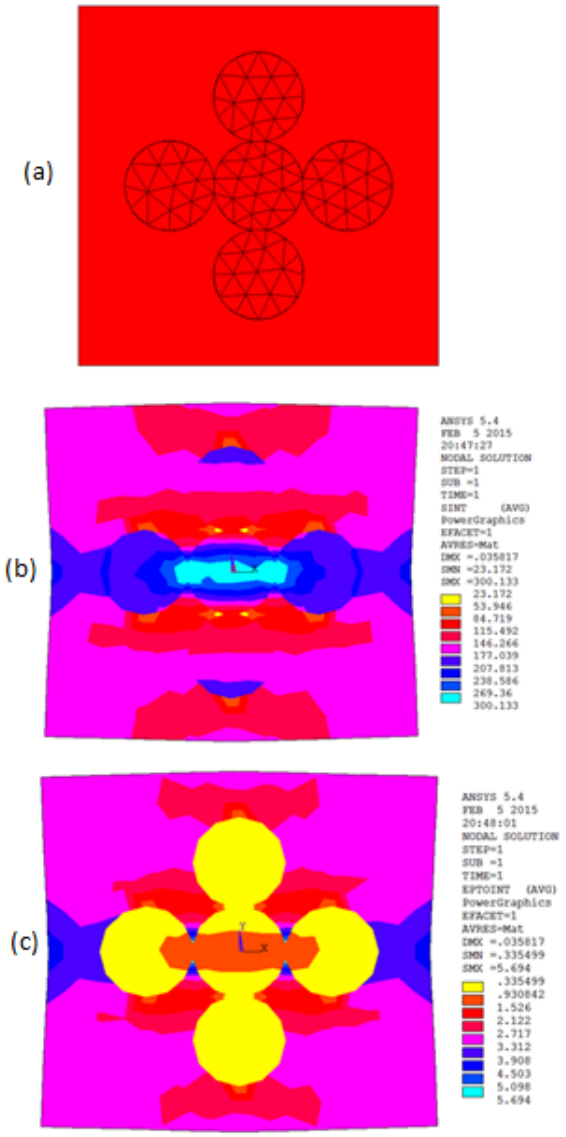

Figure 7: Finite element analysis of particle clustering

Hojo et al. [10] found that the strength of silica-filled epoxy decreased with increasing mean particle size d_p according to the relation

$$\sigma_c = \sigma_m + k(v_p) d_p^{-1/2} \quad (15)$$

where $k(v_p)$ is a constant being a function of the particle loading. This criterion holds good for small particle size, but fails for larger particles as shown in figure 9. Withal, the composite strength decreases with increasing filler-loading in the composite.

A new criterion is suggested by the author considering adhesion, formation of precipitates, particle size, agglomeration, voids/porosity, obstacles to the dislocation,

and the interfacial reaction of the particle/matrix. The formula for the strength of composite is stated below:

$$\sigma_c = \left[\sigma_m\left(\frac{1-(v_p+v_v)^{2/3}}{1-2(v_p+v_v)}\right)\right]e^{m_m(v_p+v_v)} + k(v_p)m_p d_p^{-1/2} \quad (16)$$

where v_v is the volume fraction of voids/porosity in the composite, m_m and m_p are the possion's ratios of the matrix and particulates, and $k(v_p)$ is the slope of the tensile strength against the mean particle size (diameter) and is a function of particle volume fraction v_p. The predicted strength values are within the allowable bounds of experimental strength values as shown in figure 10.

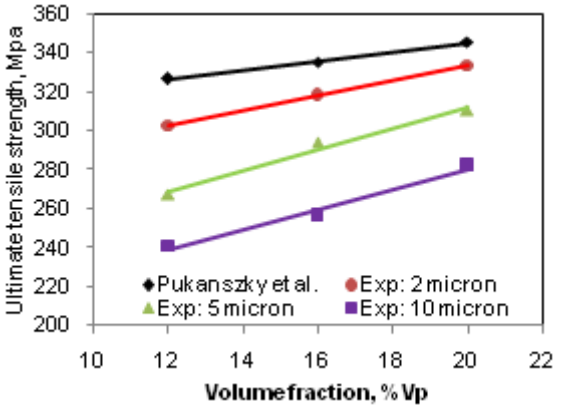

Figure 8: Comparison of Pukanszky et al criterion with experimental values

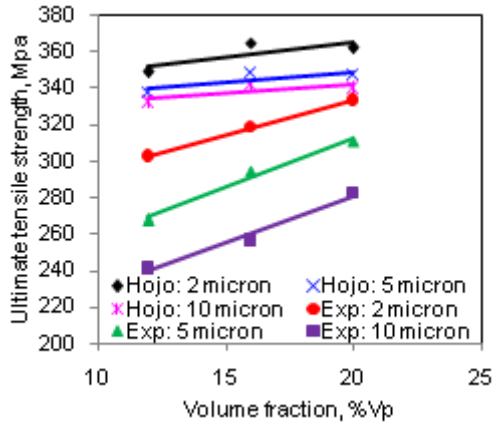

Figure 9: Comparison of Hojo criterion with experimental values

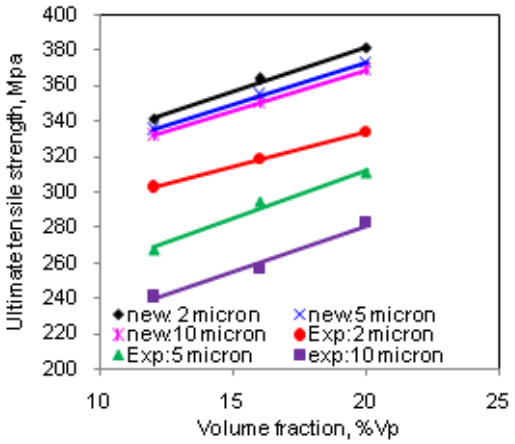

Figure 10: Comparison of proposed criterion with experimental values

4.4 Elastic Modulus

Elastic modulus (Young's modulus) is a measure of the stiffness of a material and is a quantity used to characterize materials. Elastic modulus is the same in all orientations for isotropic materials. Anisotropy can be seen in many composites. Silicon carbide (Al2O3) has much higher Young's modulus (is much stiffer) than 6061 aluminium alloy.

Ishai and Cohen [11] developed based on a uniform stress applied at the boundary, the Young's modulus is given by

$$\frac{E_c}{E_m} = 1 + \frac{1+(\delta-1)v_p^{2/3}}{1+(\delta-1)\left(v_p^{2/3}-v_p\right)} \quad (17)$$

which is upper-bound equation. They assumed that the particle and matrix are in a state of macroscopically homogeneous and adhesion is perfect at the interface. The lower-bound equation is given by

$$\frac{E_c}{E_m} = 1 + \frac{v_p}{\delta/(\delta-1) - v_p^{1/3}} \quad (18)$$

where $\delta = E_p / E_m$.

The proposed equation by the author to find Young's modulus includes the effect of voids/porosity in the composite as given below:

$$\frac{E_c}{E_m} = \left(\frac{1-v_v^{2/3}}{1-v_v^{2/3}+v_v}\right) + \left(\frac{1+(\delta-1)v_p^{2/3}}{1+(\delta-1)\left(v_p^{2/3}-v_p\right)}\right) \quad (19)$$

The results shown in table 1 indicate the rduction of Young's modulus due to porosity, particle size, debonding and particle clustering.

Table 1: Young's modulus obtained from various criteria

Criteria	Young's modulus, GPa		
	Vp =12	Vp =16	Vp =20
Ishai and Cohen (upper bound)	160.97	167.69	174.40
New proposal from Author	159.92	166.39	172.83

4.5 Weibull Statistical Strength Criterion

The tensile strength of 6061/Al_2O_3 was analysed by Weibull statistical strength criterion using Microsoft Excel software. The slope of the line, β, is particularly significant and may provide a clue to the physics of the failure. The Weibull graphs of tensile strength indicate lesser reliability for filler loading of 12% than those reliabilities of 16, and 20 (figure 11). The shape parameters, βs (gradients of graphs) are 10.193, 10.822, and 13.322 respectively, for the composites having the particle volume fraction of 12%, 16%, and 20%.

The Weibull characteristic strength is a measure of the scale in the distribution of data. It so happens that 63.2 percent of the composite has failed at σ_0. In other words, for a Weibull distribution R (=0.368), regardless of the value ofβ. With 6061/Al_2O_3, about 36.8 percent of the tensile specimens should survive at least 283.14 MPa, 302.92 MPa, and 319.49 MPa for 12%, 16%, and 20% volume fractions of Al_2O_3 in the specimens respectively. The reliability graphs of tensile strength are shown in figure 12. At reliability 0.90 the

survival tensile strength of 6061/Al_2O_3 containing 12% of volume fraction is 227.06 MPa, 16% of volume fraction is 246.05 MPa, and 20% of volume fraction is 269.83 MPa. This clearly indicates that the tensile strength increases with increase in volume fraction of Al_2O_3.

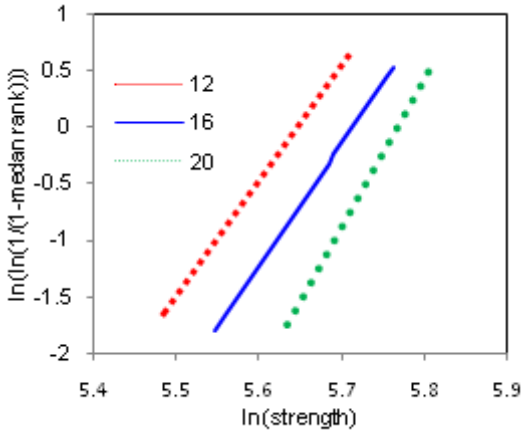

Figure 11: Weibull distribution of tensile strength

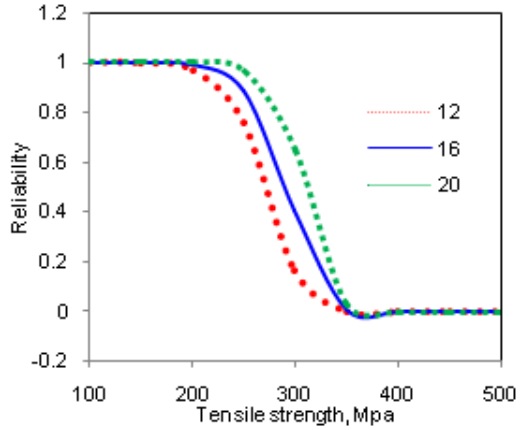

Figure 12: Reliability graphs for tensile strength of /6061/Al_2O_3.

4.5 Fracture

Fractography revealed macroscopically brittle appearance whereas microscopically local ductile and brittle mechanisms. Failure of the composite was found to occur by reinforcement cracking and particle-matrix decohesion at the interface. The fracture process in a high volume fraction (20%) aluminium/Al_2O_3 composite is very much localized. The failure path in these composites is through the matrix due to matrix cracking and the connection of these microcracks to the main crack. Sugimura and Suresh reported that the cracking of Al_2O_3 particles was a rare event for small size (≤10μm) of particles [12]. There was an incident of particle cracking in case of composite having 10μm size of particulates. The presence of Al_2O_3 reinforcement particles reduces the average distance in the composite by providing strong barriers to dislocation motion. The interaction of dislocations with other dislocations, precipitates, and Al_2O_3 particles causes the dislocation motion. The presence of voids is also observed in the composites having larger Al_2O_3 particles. The void coalescence occurs when the void elongates to the initial intervoid spacing. This contributes to the dimpled appearance of the fractured surfaces (figure 13).

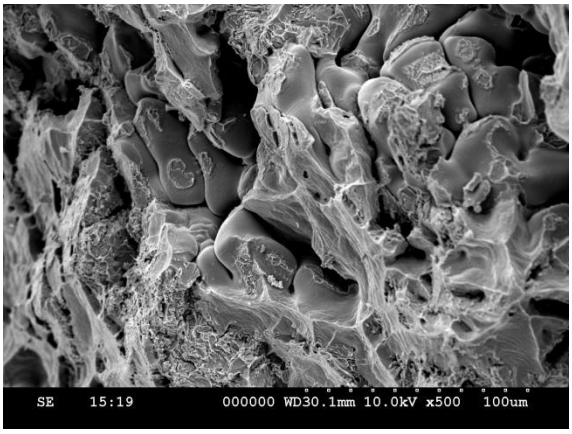

Figure 13: SEM of fracture surface of 6061/Al_2O_3 composites of 20% Vf and 10 μm particle size of Al_2O_3 in 6061.

5. Conclusions

The EDS report confirms the presence of Mg_2Si and Al2Cu precipitates in the 6061/Al_2O_3 composites. After heat treatment to the T4 condition, most of the coarse intermetallic phases such as (Al_2Cu, Mg_2Si) are dissolved to form $Al_5Cu_2Mg_8Si_6$ or $Al_4CuMg_5Si_4$ compound. The porosity of approximately 42μm was also revealed in the 6061/Al_2O_3 composite having 10μm particles. At higher volume fractions concentration, i.e., small interparticle distances, the particle-particle interaction may develop agglomeration in the composite. Non-planar cracking of particle was observed in the 6061/Al_2O_3 composite comprising 10μm particles. The tensile strength increases with increase in volume fraction of Al_2O_3, whereas it decreases with increasing particle size. The experimental values of tensile strength and Young's modulus are nearly equal to the predicted values by the new formulae proposed by the author. The FEA results confirm the occurrence of particle debonding, porosity, and clustering in the composites.

6. Acknowledgements

The author acknowledges with thanks University Grants Commission (UGC) – New Delhi for sectioning R&D project, and Tapasya Casting Private Limited – Hyderabad, and Indian Institute of Chemical Technology – Hyderabad for their technical help.

References

[1] M. Redsten, E. M. Klier, A. M. Brown, D. C. Dunand, "Mechanical properties and microstructure of cast oxide-dispersion-strengthened aluminum", Materials Science & Engineering, A: Structural Materials: Properties, Microstructure and Processing, (201), pp.88-102, 1995.

[2] T.S. Srivatsan, "Microstructure, tensile properties and fracture behavior of Al_2O_3 particulate-reinforced

aluminum alloy metal matrix composites", Journal of Materials Science, (31), pp.1375-1388, 1996.
[3] S.V. Kamat, J.P. Hirth, and R. Mehrabian, "Mechanical properties of particulate-reinforced aluminum-matrix composites", Acta Metallurgica, (37), pp.2395-2402, 1989.
[4] R. H. Pestes, S.V. Kamat, and J.P. Hirth, "Fracture toughness of Al-4%Mg/Al_2O_3 composites", Materials Science & Engineering, A: Structural Materials: Properties, Microstructure and Processing A, (189), 1994, pp. 9-14.
[5] A. Chennakesava Reddy, Essa Zitoun, "Tensile behavior 0f 6063/al2o3 particulate metal matrix composites fabricated by investment casting process", International Journal of Applied Engineering Research, (01), pp.542-552, 2010.
[6] A. Chennakesava Reddy, "Strengthening mechanisms and fracture behavior of 7072Al/Al_2O_3 metal matrix composites", International Journal of Engineering Science and Technology, (03), pp.6090-6100, 2011.
[7] Chennakesava R Alalvala, "Finite Element Methods: basic Concepts and Applications", PHI Learning Private Limited, New Delhi, 2008.
[8] A. Chennakesava Reddy, "Fracture behavior of brittle matrix and alumina trihydrate particulate composites", Indian Journal of Engineering & Materials Sciences, (5), pp 365-368, 2002.
[9] B. Punkanszky, B. Turcsanyi, F. Tudos, "Effect of interfacial interaction on the tensile yield stress of polymer composites", In: H. Ishida, editor, Interfaces in polymer, ceramic and metal matrix composites, Amsterdam: Elsevier, pp.467-77, 1998.
[10] H. Hojo, W. Toyoshima, M. Tamura, N.Kawamura, "Short- and long- term strength characteristics of particulate-filled cast epoxy resin", Polymer Engineering and Science, (14), pp 604-609, 1974.
[11] O. Ishai, I.J.Cohen, "Elastic properties of filled and porous epoxy composites", International Journal of Mechanical Sciences, (9), pp 539-546. 1967.
[12] Y. Sugimura, S. Suresh, "Effects of Al_2O_3 content on fatigue crack growth in aluminium alloy reinforced with $A_{l2}O_3$ particles", Metallurgical Transactions A, (23), pp.2231-2342, 1992.

Author Profile

Dr. A. Chennakesava Reddy, B.E., M.E (prod). M.Tech (CAD/CAM)., Ph.D (prod)., Ph.D (CAD/CAM) is a Professor in Mechanical Engineering, Jawaharlal Nehru Technological University, Hyderabad. The author has published 209 technical papers worldwide. He is the recipient of best paper awards nine times. He is recipient of Best Teacher Award from the Telangana State, India. He has successfully completed several R&D and consultancy projects. He has guided 14 Research Scholars for their Ph.D. He is a Governing Body Member for several Engineering Colleges in Telangana. He is also editorial member of Journal of Manufacturing Engineering. He is author of books namely: FEA, Computer Graphics, CAD/CAM, Fuzzy Logic and Neural Networks, and Instrumentation and Controls. Number of citations are 514. The total impact factors are 75.2545.His research interests include Fuzzy Logic, Neural Networks, Genetic Algorithms, Finite Element Methods, CAD/CAM, Robotics and Characterization of Composite Materials and Manufacturing Technologies.